AEM JOURNAL .ORG

# A Miniature Hexa-Band Antenna for Internet of Things Applications Using Six Quarter-wavelength Resonators

**Yousif Mohsin Hasan[1], Zain-Aldeen S. A. Rahman[2], and Yasir I. A. Al-Yasir [3,4]**
[1]Department of Electronic and Communication Engineering, College of Engineering, University of Al-Qadisiyah, Iraq
[2]Department of Electrical Techniques, Technical Institute/Qurna, Southern Technical University, Basra 61016, Iraq
[3]Communication and Space Systems Engineering Research Team, Manchester Metropolitan University, Manchester, UK
[4]Communications Engineering Department, Iraq University College, Basra, Iraq
Corresponding author: Yousif Mohsin Hasan (e-mail: yousif.hasan@qu.edu.iq)

**ABSTRACT** This work presents a compact, low-cost hexa-band microstrip antenna for Internet of Things (IoT) applications. The proposed hexa-band antenna is composed of simple six-$\lambda/4$ resonators to generate six resonant frequencies: GSM 1.84 GHz (1.8 - 1.89 GHz), Bluetooth 2.31 GHz (2.25 –2.375 GHz), WiMAX 3.3 GHz (3.16 - 3.47 GHz), WiFi 4.63 GHz (4.34 - 5 GHz), upper WLAN 6.1 GHz (5.8 - 6.91 GHz) and X-band 9.26 GHz (8.87 - 9.83 GHz). The proposed hexa-band antenna is fabricated using FR4 substrate with (23 × 20 × 1.6) $mm^3$ dimensions, and its measured results are presented to validate the simulated results. The results of simulations and measurements are used to examine the radiation properties, including radiation patterns, gain, efficiency, VSWR, and reflection coefficient. The proposed hexa-band antenna has a miniaturized size and good radiation performance.

**INDEX TERMS** Hexa-band antenna, Multi-band antenna, IoT, Bluetooth, GSM, WiFi, WiMAX, WLAN, X-band.

## I. INTRODUCTION

WIRELESS communications are rapidly progressing. The very small portable devices in modern wireless communications require compact multi-band antennas. A hexa-band antenna often refers to an antenna system that can operate in six different frequency bands. These antennas are widely employed in wireless communication applications to provide interoperability with several frequency bands used by different technologies or standards. In IOT, hexa-band antennas may be used to cover frequencies for GSM, Bluetooth, WiMAX, WiFi, GPS, WLAN, and other wireless protocols. They are intended to efficiently send and receive signals across these various frequency bands, thereby improving communication performance. An antenna that can function over six frequency bands is commonly referred to as a hexa-band antenna for Internet of Things (IoT) applications. Because they are meant to be connected to different networks, Internet of Things devices frequently need to be connected over a range of frequencies, such as GSM (1.9 GHz), WiFi (2.4 GHz and 5 GHz), Bluetooth (2.4 GHz), WiMAX (3.5 GHz), upper WLAN (6.4 GHz), and other applications. Effective approaches have been proposed to create multi-band antennas, such as dual-band [1]–[7], tri-band antenna [8]–[12], quad-band antenna design [13]–[17], pentaband [18], [19], and hexa-band antenna design [20]–[22]. Many researchers have designed multi-band antennas for IOT applications. In study [9], proposed a tribe-band antenna based on a split-square ring resonator and a half-ring resonator with a size of 33×22×1.6 $mm^3$ to operate at frequencies of 2.4, 3.7 and 5.8 GHz with gains of 1.43 dBi, 0.89 dBi and 1 dBi for IOT applications. In study [11], a Filtenna system with three modes for UWB, WiMAX 3.5 GHz, and WLAN 5.2 GHz with realized gains of 2.2 dBi, 2.65 dBi, and 1.92 dBi, respectively, for CR applications is presented. In [13], due to the use of four quarter-wavelength resonators to form a quad-band antenna, it operates at resonant frequencies of 1.8 GHz, 2.4 GHz, 3.35 GHz, and 5.4 GHz with gains of 1.5 dBi, 1.75 dBi, 2.5 dBi, and 3.7 dBi, respectively. A quad-band antenna with a whole-size of 25 × 40 × 1.5 mm3 resonant at 2.2 GHz, 5.7 GHz, 7.7 GHz, and 8.3 GHz for IOT, S-band, X-band, and RFID applications was presented in [14]. A quad-band antenna based on the L-shape slot, Sierpinski triangle, and circular split ring resonator (SRR) to generate operating frequency of 3.1 GHz, 5.52 GHz, 7.31 GHz, 9.72 GHz [17].

In this paper, a miniature hexa-band antenna for IoT applications is presented. The proposed multi-band antenna is a combination of a six-quarter-wavelength resonator that results in a compact size of 23 mm × 20 mm with multiple resonation behaviors. The proposed hexa-band antenna exhibits simulated (measured) operating frequencies at 1.946 GHz (1.84 GHz), 2.44 GHz (2.31 GHz), 3.497 GHz (3.3

GHz), 4.9 GHz (4.63 GHz), 6.34 GHz (6.1 GHz), and 9.65 GHz (9.26 GHz) for GSM, Bluetooth, WLAN, WiMax, and X-band applications. The structure of this paper is as follows: The steps for designing and developing the proposed hexa-band antenna based on the six resonators are presented in Section 2. A parametric study is discussed in Section 3. Section 4 presents the simulated and measured results of the proposed hexa-band antenna and compares it with other related works. The conclusion is presented in Section 5.

## II. MULTI-BAND ANTENNA DESIGN

The proposed hexa-band antenna is shown in Figure 1. The front side of the proposed antenna consists of six quarter-wavelength resonators integrated within a 50-ohm transmission feed line to ensure hexa-band functionality. The backside of the antenna shows the trapped, partial ground. The CST simulation software [23] is used for the design and optimization of the proposed multi-band antenna. FR4 substrate with a dielectric constant of 4.3 and a loss tangent of 0.02 is used to simulate the developed multi-band antenna, whose electrical size in terms of wavelength is 0.149 $\lambda$ × 0.123 $\lambda$, where $\lambda$ is the wavelength at the first resonant frequency of the entire -10 dB operating frequency range. All the optimized parameter values of the proposed hexa-band antenna are listed in Table 1.

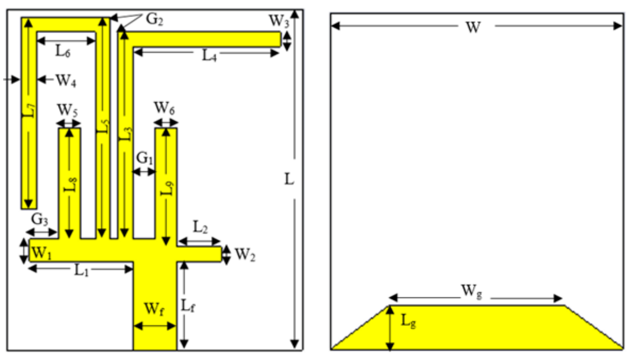


(a) (b)

FIGURE 1. Proposed hexa-band antenna (a) Front side; (b) Back side.

TABLE 1. The Parameter Values of the Proposed Hexa-Band Antenna.

| Parameter | Value(mm) | Parameter | Value(mm) |
|---|---|---|---|
| $L$ | 23 | $W$ | 20 |
| $L_1$ | 7 | $W_1$ | 1.5 |
| $L_2$ | 3 | $W_2$ | 1 |
| $L_3$ | 14 | $W_3$ | 1 |
| $L_4$ | 10 | $W_4$ | 1 |
| $L_5$ | 15 | $W_5$ | 1.5 |
| $L_6$ | 4 | $W_6$ | 1.5 |
| $L_7$ | 13 | $G_1$ | 1.5 |
| $L_8$ | 7.5 | $G_2$ | 0.5 |
| $L_g$ | 3 | $W_g$ | 18 |
| $L_f$ | 6 | $W_f$ | 3 |

The design steps for inserting the resonators to develop the multi-band antenna are shown in Figure 2. The first step of the antenna design is to insert resonator 1 and combine it with the feeding line to form Ant.1, as shown in Figure 2 (a), to generate a single-band resonant frequency of 5.191 GHz. When adding resonator 2 and also combining it with the feeding line to form Ant.2, as shown in Figure 2 (b), to provide dual-band operation at 5.257 GHz and 8.755 GHz, a tri-band operation at 2.386 GHz, 5.543 GHz, and 8.953 GHz is generated by inserting resonator 3 (Γ-shape resonator) to form Ant.3, as shown in Figure 2(c). Inserting resonator 4 (7-shape resonator) to form Ant.4 as shown in Figure 2 (d), the penta-band operation at frequencies of (2.055 GHz, 2.463 GHz, 3.981 GHz, 5.807 GHz, and 8.986 GHz) is generated. A penta-band is also achieved when resonator 5 is attached as Ant. 5 in Figure 2 (e), and the operation frequencies are (1.946 GHz, 2.441 GHz, 3.475 GHz, 5.048 GHz, and 6.379/9.085 GHz). further inserting resonator 6 to generate the proposed antenna as shown in Figure 2(f) with hexa-band operation at resonant frequencies of (1.946 GHz, 2.44 GHz, 3.497 GHz, 4.9 GHz, 6.34 GHz, and 9.65 GHz). The simulated reflection coefficient of all steps to develop the proposed antenna are indicated in Figures 3 (a) - (f). All the simulated resonance frequencies of inserting the resonators are listed in Table 2. The resonant frequencies of all quarter wavelength resonators can be predicted from bellow equation [24], [25].

$$f_n = \frac{\lambda_g}{4} = \frac{300}{4 \times L_{Rn} \times \sqrt{\epsilon_{reff}}} \tag{1}$$

Where $L_{Rn}$ represents the length of quarter-wavelength resonator and n is the number of resonator and it takes the value from 1 to 6. $\epsilon_{reff}$ represent represents the epsilon effective value of the dielectric substrate and can be found as [26], [27]:

$$\epsilon_{eff} = \frac{\epsilon_r + 1}{2} + \frac{\epsilon_r - 1}{2}[1 + \frac{12h}{W}]^{-0.5} \tag{2}$$

The length of each one of six resonators can be determine from equations (3) -(8).

$$L_{R1} = L_1 \tag{3}$$

$$L_{R2} = L_2 + W_6 \tag{4}$$

$$L_{R3} = L_3 + L_4 + G_1 \tag{5}$$

$$L_{R4} = L_5 + L_6 + L_7 + G_1 + G_2 \tag{6}$$

$$L_{R5} = L_1 - G_3 + L_g \tag{7}$$

$$L_{R6} = L_9 \tag{8}$$

Theoretical resonant frequencies are found at $f_1$ = 6.58 GHz, $f_2$ = 9.5987 GHz, $f_3$ = 2.33 GHz, $f_4$ = 1.77 GHz, $f_5$ = 3.410 GHz, and $f_6$ = 4.74 GHz which are in good agreement with the simulated values of the resonant frequencies.

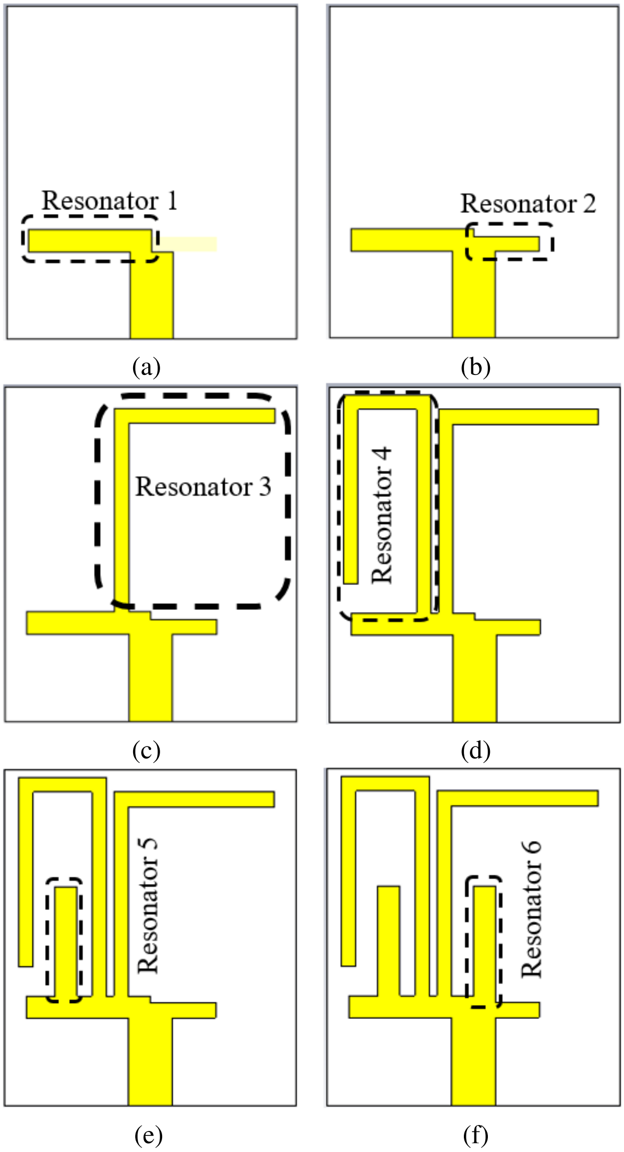


FIGURE 2. Steps to develop the proposed hexa-band antenna as: (a) Ant.1; (b) Ant.2; (c) Ant.3; (d) Ant.4; (e) Ant.5; (f) Proposed Ant.

TABLE 2. Resonant frequency for inserting different resonators to develop a hexa-band antenna.

| Resonators | $f_1$(GHz) | $f_2$(GHz) | $f_3$(GHz) | $f_4$(GHz) | $f_5$(GHz) | $f_6$(GHz) |
|---|---|---|---|---|---|---|
| 1 | 5.191 | - | - | - | - | - |
| 2 | 5.257 | 8.755 | - | - | - | - |
| 3 | 2.386 | 5.543 | 8.953 | - | - | - |
| 4 | 2.055 | 2.463 | 3.981 | 5.807 | 8.986 | - |
| 5 | 1.946 | 2.441 | 3.475 | 5.048 | 6.379/ 9.085 | - |
| 6 | 1.946 | 2.44 | 3.497 | 4.9 | 6.34 | 9.65 |

## III. ANTENNA PARAMETRIC STUDY

This section discusses how the length and width of the trapped ground ($L_g$ and $W_g$) affect the antenna performance. The reflection coefficients of the proposed hexa-band antenna for different values of the length of the trapped ground ($L_g$ = 3 mm, 4 mm, and 5 mm) and ($W_g$ = 18 mm, 19 mm, and 20 mm) are depicted in Figures 4 and 5. It shows that when you decrease the length of the ground, it improves the impedance matching of the operating frequencies. The parametric study shows the best values of Lg = 3 mm and Wg = 18 mm to achieve the hexa-band operating at 1.946 GHz, 2.44 GHz, 3.497 GHz, 4.9 GHz, 6.34 GHz, and 9.65 GHz. The reflection coefficient (S11) values of the antenna at resonant frequencies are -17.1, -26.83, -27.58, -61.54, -26, and -28.63 dB, respectively.

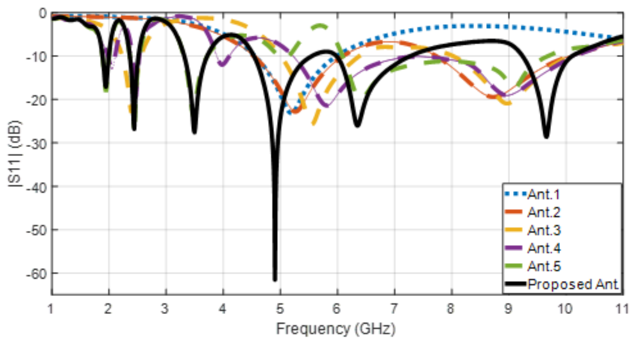


FIGURE 3. Reflection coefficient of the steps design of Antenna.

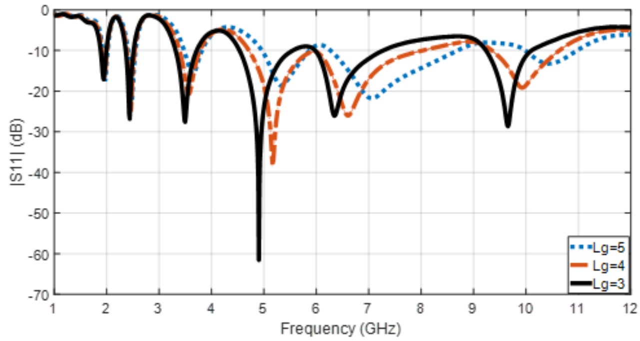


FIGURE 4. Simulated reflection coefficient of proposed hexa-band antenna at different values of $L_g$.

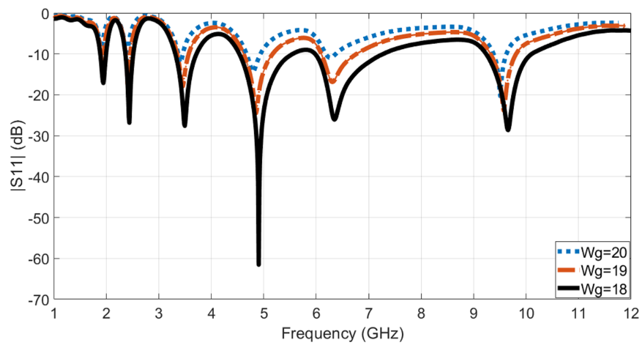


FIGURE 5. Simulated reflection coefficient of proposed hexa-band antenna at different values of $W_g$.

## IV. RESULTS AND DISCUSSIONS

Figure 6 shows the front and back sides which is fabricated the proposed hexa-band antenna using FR4 substrate and characterized by network analysis.

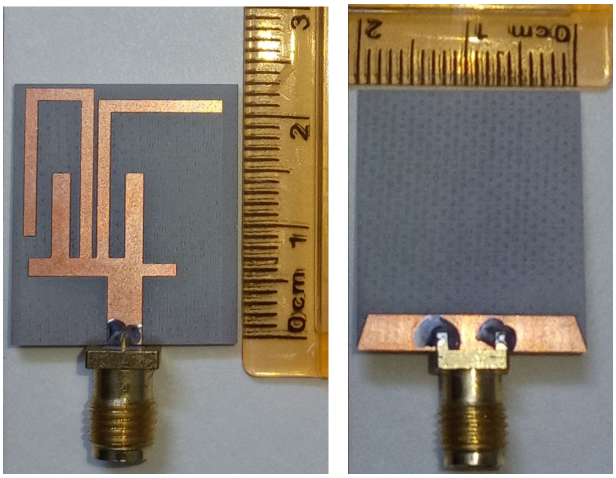

(a) (b)

FIGURE 6. Prototype of proposed hexa-band antenna (a) Front side; (b) Back side.

### A. REFLECTION COEFFICIENT

Figure 7 shows the simulated (measured) reflection coefficient of the proposed hexa-band antenna. It exhibits the simulated (measured) operating frequencies in the hexa-band of 1.946 GHz (1.84 GHz), 2.44 GHz (2.31 GHz), 3.497 GHz (3.3 GHz), 4.9 GHz (4.63 GHz), 6.34 GHz (6.1 GHz), and 9.65 GHz (9.26 GHz). The simulated -10 dB bandwidth at the six bands is 6.3% (1.88-2 GHz), 6.41% (2.364-2.518 GHz), 11.34% (3.32-3.717 GHz), 20% (4.54-5.52 GHz), 20.3% (6-7.28 GHz), and 8.91% (9.25-10.11 GHz), respectively. While the measured -10 dB bandwidth at the resonant frequencies is 6.3% (1.88-2 GHz), 6.41% (2.364-2.518 GHz), 11.34% (3.32-3.717 GHz), 20% (4.54-5.52 GHz), 20.3% (6-7.28 GHz), and 8.91% (9.25-10.11 GHz), respectively.

### B. CURRENT DISTRIBUTION

Figures 8 (a)–(d) illustrate the current distributions of the proposed hexa-band antenna at different resonant frequencies for multi-bands. Notice from the current distribution at the frequency of 6.34 GHz (Band 5) that the maximum current passes through resonator 1, as shown in Figure 8 (a). The current is consecrated on the resonator 2 at a resonant frequency of 9.65 GHz (Band 6), as shown in Figure 8 (b). The maximum current passes through resonator 3 (Γ-shape resonator) at the resonant frequency of 2.44 GHz (Band 2), as depicted in Figure 8 (c). At the fourth resonant frequency of 1.946 GHz (Band 1), the current distribution in Figure 8 (d) shows the maximum current passing through the resonator 4 (7-shape resonator). Figures 8 (e) and 8 (f) show the current distribution is centered at the fifth and sixth resonant frequencies of 3.497 GHz and 4.9 GHz (Band 3 and Band 4), respectively, for the left I-shape resonator and the right I-shape resonator (resonators 5 and 6).

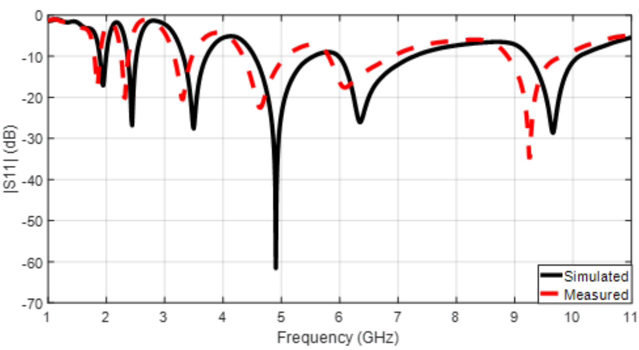


FIGURE 7. Simulated and measured reflection coefficient of proposed hexa-band antenna.

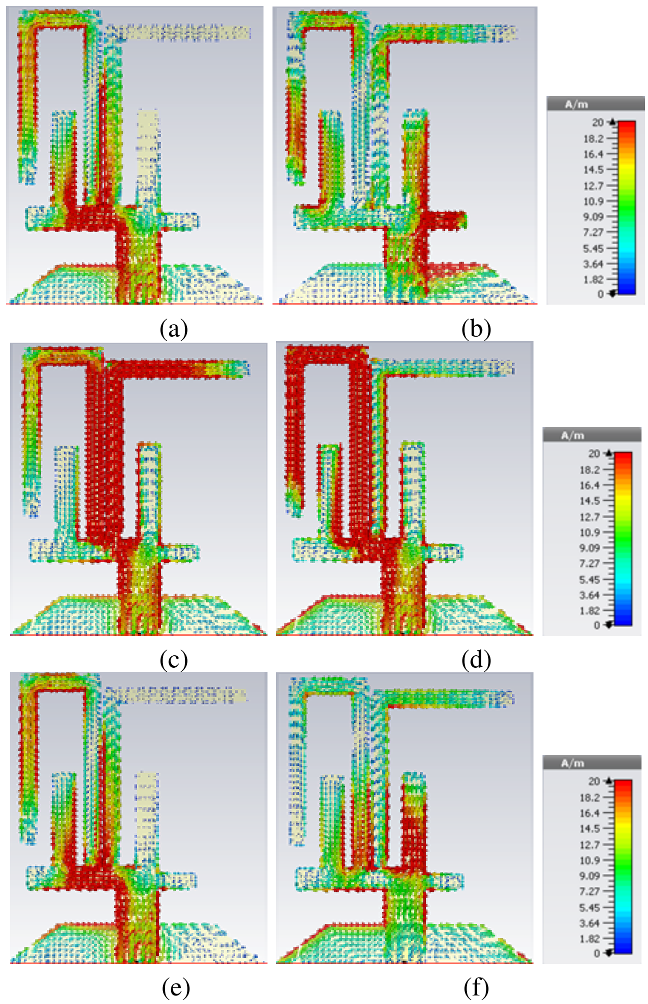


FIGURE 8. Current distribution of the proposed antenna at resonant frequencies of (a) 6.34 GHz; (b) 9.65 GHz; (c) 2.44 GHz; (d) 1.946 GHz; (e) 3.497; (f) 4.9 GHz.

### C. REALIZED GAIN AND RADIATION EFFICIENCY

Figure 9 shows the simulated (measured) realized gain of the proposed hexa-band antenna at the six operating frequencies. A peak realized gain is 1.5 dBi (1.6 dBi), 1.65 dBi (1.83 dBi), 2.2 dBi (2 dBi), 2.27 dBi (1.88 dBi), 2.75 dBi (2.44 dBi),

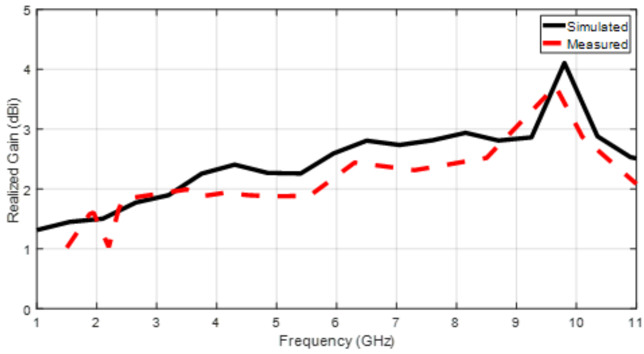


**FIGURE 9.** Simulated and measured realized gain of proposed hexa-band antenna.

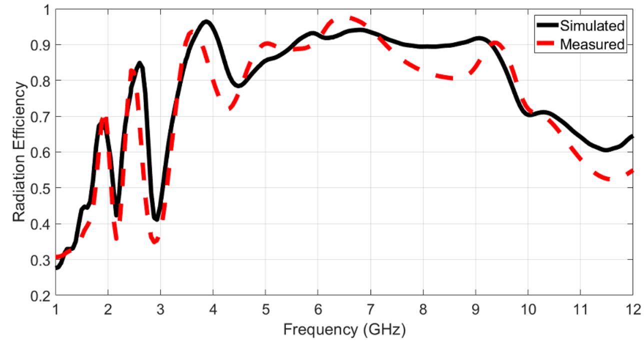


**FIGURE 11.** Simulated and measured radiation efficiency of proposed hexa-band antenna.

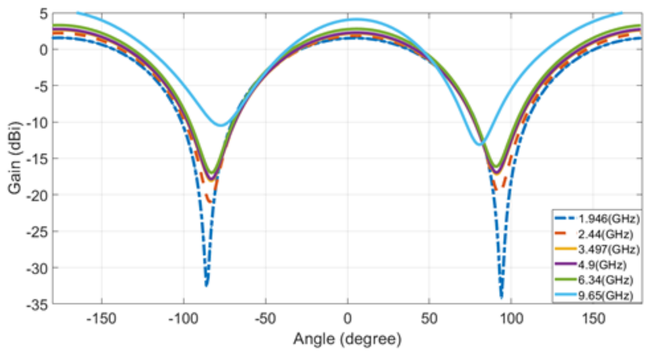


**FIGURE 12.** Gain as a function of theta (radiation pattern) with phi=90° at resonant frequencies.

and 4.1 dBi (3.7 dBi) at resonant frequencies. The simulated 3D gains of the proposed antenna at each resonant frequency are plotted as shown in Figure 10(a-f). Figure 11 shows the simulated and measured values of radiation efficiency as a function of frequency. This shows that the radiation efficiency values are higher than 70% at all resonant frequencies. All simulated and measured results for the proposed antenna are evaluated in Table 3. The reason for the slight difference between the measured results and the simulation is due to possible errors in the manufacturing process as well as the method of taking measurements using a network analyzer.

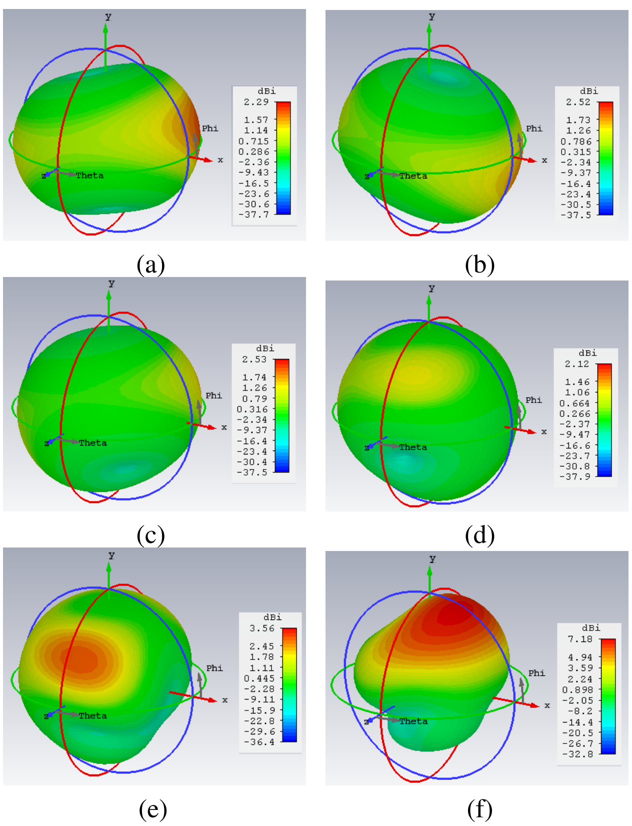


**FIGURE 10.** Simulated 3d gain of proposed hexa-band antenna as: (a) 1.946 GHz; (b) 2.44 GHz; (c) 3.497 GHz; (d) 4.9 GHz; (e) 6.34 GHz; (f) 9.65 GHz.

### D. POWER RADIATION PATTERN

Figure 12 illustrates the Cartesian gain as a function of theta (radiation pattern) of the proposed antenna at six resonant frequencies. It is supported that the proposed antenna is radiating in all directions. The simulated and measured power radiation pattern (E plane and H plane) of the proposed antenna is evaluated at the resonant frequencies of 1.946, 2.44, 3.497, 4.9, 6.34, and 9.65 GHz, and the results are shown in Figure 13(a-f). The radiation patterns at the resonant frequencies are calibrated depending on the realized gain of the proposed antenna. The omnidirectional and bidirectional in H-plane and E-plane, respectively, show this antenna can radiate in all directions, which is suitable to operate with IoT devices.

Table 4 shows a comparison of the proposed multi-band antenna with previous related studies. The comparison showed the superiority of the proposed antenna in terms of its miniature size, number of bands, low cost, good realized gain values, and high efficiency.

## V. CONCLUSIONS

A compact hexa-band antenna for IoT applications has been successfully simulated and fabricated. The simulated and measured results of the proposed hexa-band antenna have been validated. The six quarter-wavelength resonators in the proposed hexa-band antenna allow it to achieve six resonant frequencies under simulation at 1.946, 2.44, 3.497, 4.9, 6.34,

**TABLE 3.** Comparison between simulated and measured results of proposed hexa-band antenna.

| Band | Results | f(GHz) | BW(GHz) | S11(dB) | Gain(dBi) |
|---|---|---|---|---|---|
| Band 1 | Sim. | 1.946 | 1.88-2 | -17.1 | 1.5 |
| | Mea. | 1.84 | 1.8-1.89 | -17.36 | 1.6 |
| Band 2 | Sim. | 2.44 | 2.364-2.518 | -26.83 | 1.65 |
| | Mea. | 2.31 | 2.25-2.375 | -20.27 | 1.83 |
| Band 3 | Sim. | 3.497 | 3.32-3.717 | -27.58 | 2.2 |
| | Mea. | 3.3 | 3.16-3.47 | -20.66 | 2 |
| Band 4 | Sim. | 4.9 | 4.54-5.52 | -61.54 | 2.27 |
| | Mea. | 4.63 | 4.34-5 | -22.6 | 1.88 |
| Band 5 | Sim. | 6.34 | 6-7.28 | -26 | 2.75 |
| | Mea. | 6.1 | 5.8-6.91 | -17.61 | 2.44 |
| Band 6 | Sim. | 9.65 | 9.25-10.11 | -28.63 | 4.1 |
| | Mea. | 9.26 | 8.87-9.83 | -34.92 | 3.7 |

**TABLE 4.** Comparison of proposed multi-band antenna with others.

| Ref. | No. of bands | f(GHz) | BW(GHz) | Subs. | Gain (dBi) | Size ($mm^3$) |
|---|---|---|---|---|---|---|
| [28] | 2 | 0.915/ 2.45 | 0.018/ 0.13 | FR4 | 2.87/ 6.8 | 70×31×1.6 |
| [29] | 3 | 3.1/2.4/6 | 2.2/1/2 | FR4 | 1/1.6/2.2 | 17×33×1.6 |
| [30] | 3 | 2.3/3.3/6.5 | 1/0.7/1.9 | NA | 1.4/2/4.1 | 16×25×1.6 |
| [31] | 3 | 2.6/3.8/5.3 | 1.1/1.2/0.6 | FR4 | 2.9/2.5/3.8 | 86×61×1.6 |
| [32] | 3 | 2.45/3.5/ 5.8 | 0.39/0.39/ 0.76 | RO4350 | 6.3/7.4/ 8.7 | 26×25×1.5 |
| [14] | 4 | 2.2/5.7/ 7.7/8.3 | 0.5/1.1/ 0.3/0.1 | RT5880 | 1.4/3.3/ 6.3/3.5 | 25×40×1.5 |
| [33] | 4 | 0.8/5.8/ 8.5/11.4 | 0.3/3.2/ 2.9/1.9 | Dual substrate | -3/1.2/ 0.2/2 | 50×60×3 |
| [13] | 4 | 1.8/2.4/ 3.3/5.4 | 0.2/0.2/ 0.6/0.65 | FR4 | 1.5/1.7/ 2.5/3.7 | 32×15×1.6 |
| [34] | 5 | 0.7/1.4/ 2.1/3.8/6 | 0.4/0.1/ 0.4/3/0.4 | FR4 | 1.1/1.3/ 2/1.8/1.6 | 30×30×1.6 |
| [35] | 5 | 1.5/2.9/ 3.8/4.5/5 | 0.07/0.06/ 0.1/0.12/0.14 | FR4 | 2.5/3.5/ 1/1.8/3.8 | 36×30×1.6 |
| [36] | 5 | 2.05/3.65/5.6 /6.47/7.89 | 1.2/1.36/0.98 /0.41/0.67 | FR4 | 2.1/4.4/1.1 /2.9/5.2 | 48×58×1.3 |
| This work | 6 | 1.84/2.31/ 3.3/4.63/ 6.1/9.26 | 0.09/0.125/ 0.31/0.66/ 1.11/0.96 | FR4 | 1.6/1.83/ 2/1.88/ 2.44/3.7 | 23×20×1.6 |

and 9.65 GHz with S11 < -10 dB bandwidth: 6.3% (1.88-2 GHz), 6.41% (2.364-2.518 GHz), 11.34% (3.32-3.717 GHz), 20% (4.54-5.52 GHz), 20.3% (6-7.28 GHz), 8.91% (9.25-10.11 GHz), respectively. The antenna operates in measurements at 1.84, 2.31, 3.3, 4.63, 6.1, and 9.26 GHz with S11 < -10 dB bandwidth: 4.89% (1.8-1.89 GHz), 5.41% (2.25-2.375 GHz), 9.39% (3.16-3.47 GHz), 14.25% (4.34-5 GHz), 18.2% (5.8-6.91 GHz), 10.36% (8.87-9.83 GHz), respectively. The proposed antenna has good impedance matching and radiation pattern at the resonant frequencies, and it is suitable to cover GSM, Bluetooth, WLAN, WiFi, WiMAX, and X-band applications.

## REFERENCES


[1] W. M. Abdulkawi, A. F. A. Sheta, I. Elshafiey, and M. A. Alkanhal, "Design of low-profile single-and dual-band antennas for iot applications," Electronics, vol. 10, no. 22, p. 2766, 2021.

[2] Y. M. Hasan, A. S. Abdullah, and F. M. Alnahwi, "Dual-port filtenna system for interweave cognitive radio applications," Iranian Journal of Science and Technology, Transactions of Electrical Engineering, vol. 46, no. 4, pp. 943–958, 2022.

[3] D. Fazal and Q. U. Khan, "Dual-band dual-polarized patch antenna using characteristic mode analysis," IEEE Transactions on Antennas and Propagation, vol. 70, no. 3, pp. 2271–2276, 2021.

[4] S. Muzaffar, D. Turab, M. Zahid, and Y. Amin, "Dual-band uwb monopole antenna for iot applications," Engineering Proceedings, vol. 46, no. 1, p. 29, 2023.

[5] P. Pradeep, J. S. Kottareddygari, and C. S. Paidimarry, "Design of a dual-band monopole antenna for internet of things and sub-6 ghz 5g applications," in 2024 IEEE Wireless Antenna and Microwave Symposium (WAMS). IEEE, 2024, pp. 1–4.

[6] K. N. Ketavath, "Dual-band crescent-shaped slot patch antenna for wireless communications and iot applications," Microwave and Optical Technology Letters, vol. 65, no. 8, pp. 2392–2398, 2023.

[7] M. B. Hussain, M. Butt, Z. Nadeem, M. Zahid, and Y. Amin, "Design of dual-band microstrip patch antenna for wireless local area network applications," Engineering Proceedings, vol. 46, no. 1, p. 3, 2023.

[8] S. Ahmad, H. Boubakar, S. Naseer, M. E. Alim, Y. A. Sheikh, A. Ghaffar, A. J. A. Al-Gburi, and N. O. Parchin, "Design of a tri-band wearable antenna for millimeter-wave 5g applications," Sensors, vol. 22, no. 20, p. 8012, 2022.

[9] D. H. Abdulzahra, F. Alnahwi, A. S. Abdullah, Y. I. Al-Yasir, and R. A. Abd-Alhameed, "A miniaturized triple-band antenna based on square split ring for iot applications," Electronics, vol. 11, no. 18, p. 2818, 2022.

[10] N. Alaoui, B. A. Amel, and Z. Aya, "Tri-band frequency reconfigurable antenna for wireless applications." Instrumentation, Mesures, Métrologies, vol. 23, no. 2, 2024.

[11] Y. Hasan, A. Abdullah, and F. Alnahwi, "Three-modes, reconfigurable filtenna system with uwb, wimax, and wlan states for cognitive radio applications," International Journal on Communications Antenna and Propagation (IRECAP), vol. 14, no. 1, pp. 15–23, 2024.

[12] S. K. Sharma, T. Khan, and A. P. Singh, "Tri-band antenna with metasurface-based ground plane for sub-6 ghz 5g and 6g wpt applications," Journal of Electromagnetic Waves and Applications, pp. 1–11, 2024.

[13] S. Thiruvenkadam and E. Parthasarathy, "Compact multiband monopole antenna design for iot applications," Journal of Electromagnetic Waves and Applications, vol. 37, no. 5, pp. 629–643, 2023.

[14] W. Ali, N. Nizam-Uddin, W. M. Abdulkawi, A. Masood, A. Hassan, J. Abdul Nasir, and M. A. Khan, "Design and analysis of a quad-band antenna for iot and wearable rfid applications," Electronics, vol. 13, no. 4, p. 700, 2024.

[15] A. Raj and D. Mandal, "Design and performance analysis of graphene integrated cpw fed fractal antennae for 5g mm-wave and ground based navigation applications," MAPAN, pp. 1–27, 2024.

[16] A. K. Yadav, S. Lata, S. K. Singh, A. K. Singh, T. Sharan, and M. Masri, "Design and analysis of cpw-fed antenna for quad-band wireless applications," Journal of Electronic Materials, vol. 52, no. 7, pp. 4388–4399, 2023.

[17] T. Ali, M. S. Aw, and R. C. Biradar, "A fractal quad-band antenna loaded with l-shaped slot and metamaterial for wireless applications," International Journal of Microwave and Wireless Technologies, vol. 10, no. 7, pp. 826–834, 2018.

[18] A. K. Yadav, S. Lata, and S. K. Singh, "Design and investigation of a double-damru (pellet drum)-shaped cpw-fed microstrip patch antenna for 5g wireless communications," Journal of Electronic Materials, vol. 52, no. 7, pp. 4400–4412, 2023.

[19] H. Wang, X. Liu, X. Yang, Z. Fang, R. Zhang, and Y. Wang, "Penta-band rectangular slot antenna for multi-function wireless communication with linear and circular polarizations," International Journal of Microwave and Wireless Technologies, vol. 15, no. 8, pp. 1382–1391, 2023.

[20] K. Srivastava, A. Kumar, and B. K. Kanaujia, "Design of compact penta-band and hexa-band microstrip antennas," Frequenz, vol. 70, no. 3-4, pp. 101–111, 2016.

[21] V. Jayaprakash, D. Chandu, R. K. Barik, and S. Koziel, "Compact substrate-integrated hexagonal cavity-backed self-hexaplexing antenna for sub-6 ghz applications," IEEE Access, 2024.

[22] B.-J. Niu and J.-H. Tan, "Hexa-band siw cavity antenna system integrating two antennas with high isolation," Electronics Letters, vol. 55, no. 9, pp. 505–506, 2019.

[23] CST, "Computer simulation technology based on fit method," 2017.

[24] Y. M. Hasan, A. S. Abdullah, and F. M. Alnahwi, "Uwb filtenna with reconfigurable and sharp dual-band notches for underlay cognitive radio applications." Progress in Electromagnetics Research C, vol. 120, pp. 45–60, 2022.

[25] Y. M. Hasan, K. D. Rahi, and A. A. Mahmood, "Rectangular antenna with dual-notch band characteristics for uwb applications," in AIP Conference Proceedings, vol. 2591, no. 1. AIP Publishing, 2023, p. 020032.

[26] C. A. Balanis, Antenna theory: analysis and design. John wiley & sons, 2016.
[27] Y. M. Hasan, "A compact monopole slotted patch-antenna for uwb applications," Progress In Electromagnetics Research C, vol. 151, pp. 65–71, 2025.
[28] M. Najumunnisa, A. S. C. Sastry, B. T. P. Madhav, S. Das, N. Hussain, S. S. Ali, and M. Aslam, "A metamaterial inspired amc backed dual band antenna for ism and rfid applications," Sensors, vol. 22, no. 20, p. 8065, 2022.
[29] M. Karthikeyan, R. Sitharthan, T. Ali, and B. Roy, "Compact multiband cpw fed monopole antenna with square ring and t-shaped strips," Microwave and Optical Technology Letters, vol. 62, no. 2, pp. 926–932, 2020.
[30] P. Jha, A. Kumar, A. De, and R. K. Jain, "Cpw-fed metamaterial inspired compact multiband antenna for lte/5g/wlan communication," Frequenz, vol. 76, no. 7-8, pp. 401–407, 2022.
[31] L. Wang, J. Yu, T. Xie, and K. Bi, "A novel multiband fractal antenna for wireless application," International Journal of Antennas and Propagation, vol. 2021, no. 1, p. 9926753, 2021.
[32] R. Li, C. Wu, X. Sun, Y. Zhao, and W. Luo, "An ebg-based triple-band wearable antenna for wban applications," Micromachines, vol. 13, no. 11, p. 1938, 2022.
[33] A. Kumar and A. P. S. Pharwaha, "Development of a modified hilbert curve fractal antenna for multiband applications," IETE Journal of Research, vol. 68, no. 5, pp. 3597–3606, 2022.
[34] A. Desai, R. Patel, T. Upadhyaya, H. Kaushal, and V. Dhasarathan, "Multiband inverted e and u shaped compact antenna for digital broadcasting, wireless, and sub 6 ghz 5g applications," AEU-International Journal of Electronics and Communications, vol. 123, p. 153296, 2020.
[35] R. Patel, A. Desai, T. Upadhyaya, T. K. Nguyen, H. Kaushal, and V. Dhasarathan, "Meandered low profile multiband antenna for wireless communication applications," Wireless Networks, vol. 27, pp. 1–12, 2021.
[36] H. Zhangfang, X. Wei, L. Yuan, H. Yinping, and Z. Yongxin, "Design of a modified circular-cut multiband fractal antenna," The Journal of China Universities of Posts and Telecommunications, vol. 23, no. 6, pp. 68–75, 2016.

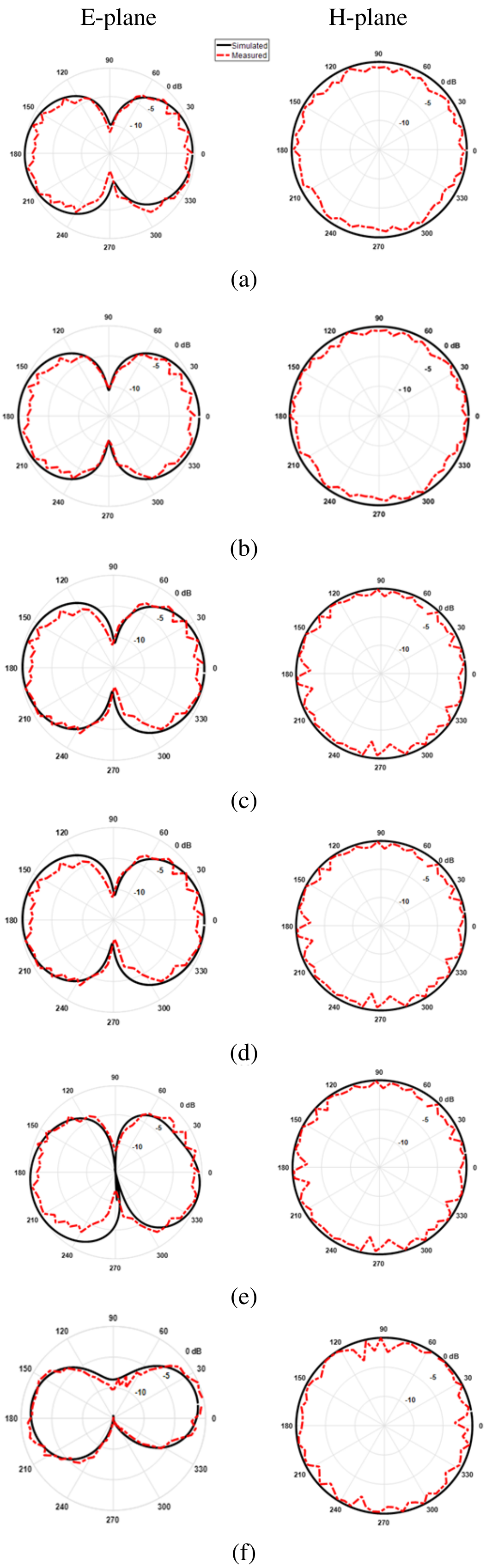


**FIGURE 13.** Simulated and measured power pattern of the proposed antenna at the resonant frequencies of (a) 1.946 GHz; (b) 2.44 GHz; (c) 3.497 GHz; (d) 4.9 GHz; (e) 6.34; (f) 9.65 GHz.